A Space-Variant Luminance Map based Color Image Enhancement

Sungmok Lee, Homin Kwon, Hagyong Han, Gidong Lee, and Bongsoon Kang, *Member*, IEEE

Abstract — *Improvement of image quality has been highly demanding for users in digital imaging systems. A variety of image enhancement algorithms has been developed to control image enhancement factors. This paper presents a color image enhancement method that makes use of a space-variant luminance map (SVLM) for the local brightness characterization. Two-dimensional gamma correction combined with the SVLM is developed to increase the intensity at the dark region and vice versa at the bright region in the luminance domain. The enhanced luminance information is applied to the adaptive contrast enhancing process and the linear color restoration. The proposed algorithm reveals details of the input image as well as minimizes loss of the edge sharpness in the non-uniform and low illumination conditions. The developed enhancement process resulted in the lowest absolute mean brightness error (AMBE) in a low-complexity fashion. A series of experimental results are discussed in terms of visual quality, the enhancement performance, and the complexity.*

Index Terms — Dynamic Range Extension, Color Image Enhancement, Contrast Enhancement, Color Restoration

I. INTRODUCTION

Improvement of image quality has been highly demanding for users in digital imaging systems including HDTV, LCD display, digital photography, etc. The image quality is mostly deteriorated by several reasons such as the limited bit-resolution, the narrow dynamic range, the insufficient acquisition time [1]. These affect the human visual perception in terms of over-saturation/under-saturation, the blurring, and color distortion. Image enhancement algorithms including homomorphic filtering methods, histogram based techniques, and transform based techniques [2] have been studied to provide better quality for users. In order to improve the visual quality of the input image captured in dynamic illumination environments, luminance and color information is characterized in terms of the spatial frequency [3]. This characteristic leads complexity/performance tradeoffs between the global and the local in the spatial perspective. In particular, the transfer function design that increases the visual perception is an important key to perform the image enhancement.

Such as histogram equalization (HE) technique makes use of the probability distribution of the input intensity to remap into the defined gray levels. [4]. According to the entire remapping, the HE shows the acceptable performance under uniform illumination. The adaptively partitioned HE was reported to preserve the brightness and improve the contrast [5]. However, additional corrections are required to preserve the color consistency. Under non-uniform illumination, the current HE techniques challenge the over enhancement. A gamma correction scheme using the single nonlinear curve has been successfully applied in image contrast enhancement [6]. The achievable performance depends on the optimal gamma value which is non-trivial task. Given the non-uniform illumination, the gamma correction challenges the over-saturation/under-saturation. In order to combine with the local characteristic on the gamma correction, the dynamic range optimization (DRO) was developed based on a bilateral filter. Due to the significant computational complexity of the filtering, the DRO may not appropriate for real-time applications. In addition, the color constancy must be considered because of the color distortion caused by the contrast enhancement in the luminance space [7].

In other hand, Tao and Asari reported the adaptive and integrated neighborhood dependent approach for nonlinear enhancement (AINDANE) for low and non-uniform illuminance conditions [8]. The separated adaptive luminance and contrast enhancement processes are developed to maintain the dependency of image brightness. Although the combined method is useful to refine the image quality, the performance is focused on the low luminance condition. The transfer function has the lack of the local characteristic as well as the lack of the bright region improvement. Retinex based algorithms considering the lightness and color in the human visual perception perspective have been advanced in terms of local contrast enhancement and lightness/color rendition. Z. Rahman *et al.* reported the multiscale retinex with color restoration (MSRCR) that makes use of the logarithmic transfer functions associated with the spatial convolution performing at individual R/G/B spectral bands [9]. The high computational complexity has been still an open issue.

In this paper, we propose a color image enhancement method that makes use of a space-variant luminance map (SVLM) including the local brightness characteristic. The SVLM is calculated using the local average luminance in the down-scaled and up-scaled input intensity image where the single Gaussian masking is carried out. Combining the SVLM with the conventional gamma correction, two-dimensional gamma correction is developed to increase the

Sungmok Lee is with Department of Electronics Engineering, Dong-A University, Busan, South Korea

Homin Kwon is with TruDef Research. Inc, San Diego, CA, USA

Hagyong Han is with BK21 High Performance Multimedia Team, Dong-A University, Busan, South Korea

Gidong Lee is with Department of Electronics Engineering, Dong-A University, Busan, South Korea

Bongsoon Kang is with Department of Electronics Engineering, Dong-A University, Busan, South Korea (e-mail: bongsoon@dau.ac.kr)

Manuscript received 10/08/10
Current version published 12/23/10
Electronic version published 12/30/10.

intensity at the dark region and vice versa at the bright region in the luminance domain. The enhanced luminance information is applied to the adaptive contrast enhancing process developed in [8]. We empirically customize the adaptive factor and follow the linear color restoration used in [8]. For the performance comparison, the MSRCR, the AINDANE and the DRO are considered in terms of the color image, the absolute mean brightness error (AMBE), and the required computational complexity. The experimental results are discusses based on the characteristics of each algorithm. The proposed method combined with the local characteristic reveals details of the input image as well as minimizes loss of the edge sharpness in the non-uniform and low illumination conditions. The developed enhancement process resulted in the lowest AMBE when compared with other algorithms. The down/up scaled Gaussian masking derives the benefit of the complexity reduction for the local brightness characterization.

The paper is organized as follows. Section II presents the proposed color image enhancement method including the luminance enhancement, the contrast enhancement, and the color restoration. In Section III, a series of simulation results is discussed at the varying illuminance conditions and the performances are compared. Section IV includes concluding remarks.

II. The Color Image Enhancement Algorithms

In this section, we present the SVLM which extracts local luminance information using the spatial convolution in a low-complexity fashion. The performance is described in terms of the transfer function of the intensity and the frequency response of the Gaussian mask. The SVLM is seamlessly integrated to achieve the luminance enhancement. The adaptive contrast enhancement developed in [8] is effectively customized to preserve details of the input image. More details are in the following.

A. Space-variant Luminance map

The input RGB color image is converted to an intensity image using (1)

$$I(x,y) = 0.299 \times R(x,y) + 0.587 \times G(x,y) + 0.114 \times B(x,y) \quad (1)$$

where *R(x,y)*, *G(x,y)* and *B(x,y)* represent the Red, the Green and the Blue, respectively, for the pixel at location *(x,y)*. *I(x,y)* represents the intensity (luminance) value of the each pixel of the intensity image. The intensity image is low-pass filtered using a 2-D discrete Gaussian filter to estimate its illuminance as expressed

$$L(x,y) = \sum_{m=0}^{M-1}\sum_{n=0}^{N-1} I(x,y)\,Gaussian(x+m, y+n) \quad (2)$$

where *L(x,y)* represents the estimated illuminance value and the *Gaussian(x,y)* represents the 2-D Gaussian function with size m by n. The *Gaussian(x,y)* is defined as

$$Gaussian(x,y) = q \cdot e^{\left(\frac{-(x^2+y^2)}{c^2}\right)} \quad (3)$$

where *q* is used to normalize the Gaussian function by

$$\iint q \cdot e^{\left(\frac{-(x^2+y^2)}{c^2}\right)} dxdy = 1 \quad (4)$$

c is the scale (Gaussian surround scale constant) that determines the size of the neighborhood. Fig. 1 illustrates a block diagram of the multiple Gaussian masking used for the SVLM.

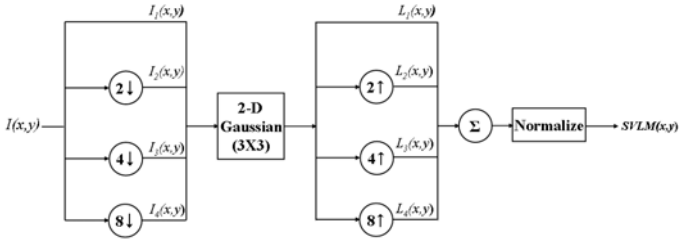

Fig. 1 A block diagram of the single Gaussian mask used for SVLM calculation.

For the computation efficiency, we used the single Gaussian mask to extract the local characteristic of the input intensity instead of employing several down-scaled sizes of the input intensity image such as 1/2,1/4,1/8 each width and height. The down-scaled convolution images are restored to the input image sizes (x2, x4, and x8) using the bicubic interpolation method [10]. The normalization is obtained from

$$SVLM(x,y) = \frac{L_1(x,y) + L_2(x,y) + L_3(x,y) + L_4(x,y)}{4} \quad (5)$$

We characterized the performance of the SVLM in the frequency response perspective. The 2-D Circular Zone Plate (CZP) method was employed as the input signals. The resolution of the input signals is 2048 x 2048. Fig. 2 shows the frequency response comparison between the proposed SVLM and the multi-Gaussian filter (MGF) (mask size : 3x3 ~ 9x9).

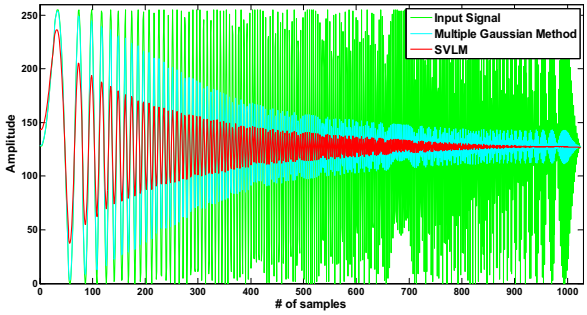

Fig. 2 The frequency response comparison of the proposed SVLM and the multiple Gaussian masking in the spatial domain method.

As the spatial frequency increases, the SVLM more attenuates the frequency response than the MGF does in the spatial domain. The attenuated frequency property is capable of accelerating the performance of the edge enhancement in the perspective of the local brightness characteristic. Fig. 3 shows the comparison between the input intensity image and its output of the SVLM. As shown in Fig. 3(b), the input intensity image is low-pass filtered associated with the local luminance of the neighboring pixels.

(a) (b)

Fig. 3 Example of the SVLM: (a) the input image and (b) SVLM.

A. Luminance Enhancement

We propose the luminance enhancement using the combination of the 2D exponential gamma correction fed by the SVLM. The pertinent local dependency obtained from the SVLM effectively enhance the luminance of the input image. Combining the input intensity *I(x,y)* with the power factor of the SVLM, the 2D gamma correction can be expressed as

$$O(x,y) = 255\left(\frac{I(x,y)}{255}\right)^{\gamma}, \quad \gamma = \alpha^{\left(\frac{128 - SVLM(x,y)}{128}\right)} \qquad (6)$$

where *O(x,y)* represents the luminance enhancement intensity value, and γ represents the exponential value including the dynamic local characteristic for the luminance enhancement.

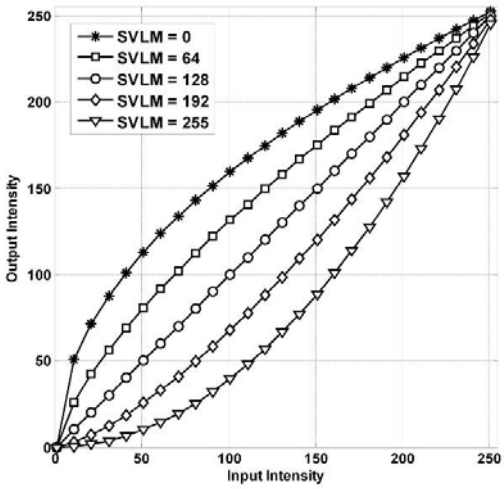

Fig. 4 Transfer function of the Luminance Enhancement: global exponential value α = 0.5 (asterisks with solid line for SVLM = 0, squares with solid line for SVLM = 64, circles with solid line for SVLM = 128, diamonds with solid line for SVLM = 192, and triangle with solid line for SVLM = 255).

The global image dependency is expressed by the value of the parameter α from 0 to 1. For case of the low contrast images, α is turned towards zero as strongly enhanced. α is turned toward *0* when no correction is required. The local dependency is obtained from the *SVLM(x,y)* containing the blurred intensity of the input image. Fig. 4 shows the transfer function of the luminance enhancement at α = 0.5. The enhancing curve depicts the exponential increase with the integer power at SVLM greater than 128, linear at SVLM equal to 128, the exponential increase with the rational power at SVLM lesser than 128. The transfer function shown in Fig. 4 enhances the light of the dark regions in the input image due to the low SVLM value. The case of input value is 100 and SVLM value is 64, the output value is generated 130. The bright regions become dark due to the high SVLM value. The case of same input value and SVLM value is 192, the output value is generated 65.

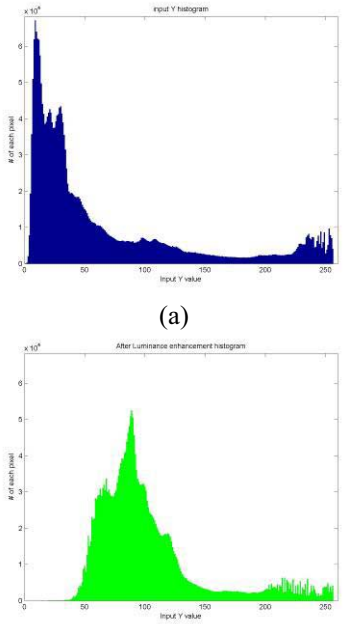

(a)

(b)

Fig. 5 Comparison between the input image luminance and after the luminance enhancement: (a) input histogram and (b) after luminance enhancement.

Fig 5 shows the comparison between the input image luminance and after the luminance enhancement. It is seen that the enhancement process largely increases the luminance of the dark pixels and moderately decreases the luminance of the bright pixels. Our luminance enhancement leads to the more visible effect in the shadow and highlight regions.

B. Contrast Enhancement

Using the enhanced luminance information above, we enhance the contrast. The visual quality improvement is accomplished using the *SVLM(x,y)* in the adaptive contrast

enhancing process [8] as show in (7)-(9):

$$S(x,y)=255\left[\frac{O(x,y)}{255}\right]^{E(x,y)} \tag{7}$$

where $E(x,y)$ is

$$E(x,y)=r(x,y)^{p}=\left[\frac{SVLM(x,y)}{O(x,y)}\right]^{P} \tag{8}$$

and the adaptive factor P is

$$P=\begin{cases}2 & for\ \ \sigma \le 40\\ -0.025\sigma+3 & for\ \ 40<\sigma\le 80\\ 1 & for\ \ \sigma>80\end{cases}. \tag{9}$$

In (9) $r(x,y)$ is the ratio, and the P is an image-dependent parameter containing the standard deviation of an image to tune the contrast enhancing. The standard deviation σ is calculated from the $I(x,y)$ indicating the contrast level of the input intensity image. The customized factor in (9) empirically obtained in our experiments. The contrast enhancing process in (7)-(9) produces the output image pixels depending on their neighboring pixels. The luminance of the dark regions becomes boosted and the luminance of the bright regions becomes attenuated. Therefore, the image contrast and fine details are effectively enhanced without degrading the image quality

C. Color Restoration

The enhanced image processed in the above is converted to the RGB space as written in (10).

$$R'=S(x,y)\frac{R(x,y)}{O(x,y)}\lambda,\ G'=S(x,y)\frac{G(x,y)}{O(x,y)}\lambda,\ B'=S(x,y)\frac{B(x,y)}{O(x,y)}\lambda \tag{10}$$

where', G' and B' are the RGB values of the enhanced color image. λ is the adjusting factor for the color hue [11].

III. Simulation Results and Discussion

In this section, we discuss the performance in terms of the intensity histogram analysis, the simulated color image, the absolute mean brightness error, and the complexity. The proposed method is compared with the AINDANE, the MSRCE, and the DRO as the baseline performance. The gamma correction and the GHE are considered for the performance comparison at the varying luminance conditions as well.

A. Histogram Analysis

Fig. 6 shows the performance comparisons of the intensity Histogram. Given the input image as shown in Fig. 6(a), its intensity histogram is drawn in Fig. 6(b). Fig. 6(c) depicts the intensity histogram processed by the proposed method, in which the shadow region moves to the right centered about 25 and such the bright region as sky is less changed above 100. Fig. 6(d) depicts the intensity histogram processed by the AINDANE. It can be seen that the shadow region is a little biased to the dark ranging 0 to 50 and the sky region moves to the bright region from 100-200 to 125-200 whose peak moved from 125 to 150. This indicates that the AINDANE performs less in the dark region and cause the over enhancement in the bright region against the proposed method. Fig. 6(e) depicts the intensity histogram of the MSRCR. The considerable change occurs due to the redistribution of the shadow region from 0-50 to 0-100. The peak of the bright region remains as it is. Fig. 6(f) depicts the intensity histogram of the DRO. The shadow region moves to the bright region about 0~70, missing the dark pixels. This can cause the significant contrast of the input image. Therefore, it can be said that the proposed method exhibits the effective image enhancement under the non-uniform and low illumination conditions.

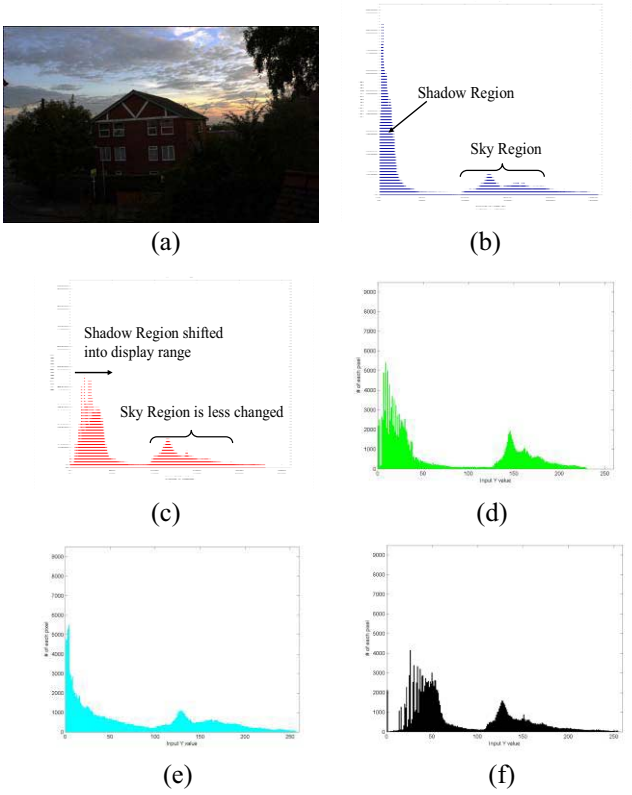

Fig. 6 Histogram analysis: (a) the input image without enhancement, (b) the intensity histogram of the input image, (c) the intensity histogram processed by the proposed algorithm, (d) the intensity histogram processed by the AINDANE, (e) the intensity histogram processed by the MSRCR, and (f) the intensity histogram processed by the DRO.

B. Simulation Results

The proposed method was applied to enhance a large number of digital images for the performance evaluation. HE, global gamma correction (GGC), DRO, AINDANE, and MSRCR are considered to compare the performance. Fig. 7 shows the results for a non-uniform illumination image. Fig. 7(a) shows the input image, Fig. 7(b) shows the output image processed by the global gamma correction (γ=0.5), respectively. The underexposed regions in Fig. 7(b) became

lighter and the details more noticeable. However, the face and the sky region were shown overexposed. Fig. 7(c) shows the output image processed by the HE. Due to the lack of the color correction process, it is excessively enhanced compared to other algorithms. Fig. 7(d) shows the output image processed by the DRO. From the use of the single-scale bi-lateral filter, the output image gives loss of details and the blur effect. Fig. 7(e) shows the output image processed by the AINDANE. While details of the image are shown using the separated enhancing processes, the color regions in tree and sky become lighter. Fig. 7(f) shows the output image processed by the MSRCR. Although the MSRCR gives the strong contrast enhancement, incorrect lightness, color noise and halo artifact are shown. In particular, the sky regions are bleached out. Fig. 7(g) shows the output image processed by the proposed method (γ=0.5). The output image shows the best quality when compared with other output images. It includes fine details, well-balanced contrast and luminance across the whole image, and natural color rendition of appropriate color saturation. In particular, details of both low-light and high-light regions are effectively enhanced. This achievement comes from the local contrast correction using the SVLM.

(a)

(b)

(c)

(d)

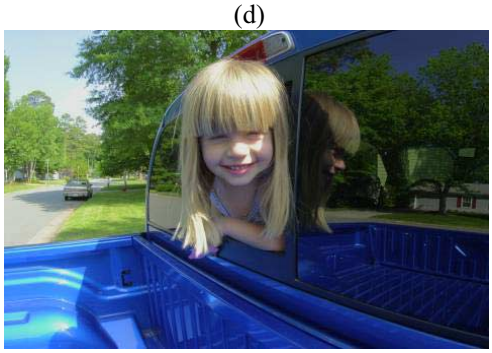

(e)

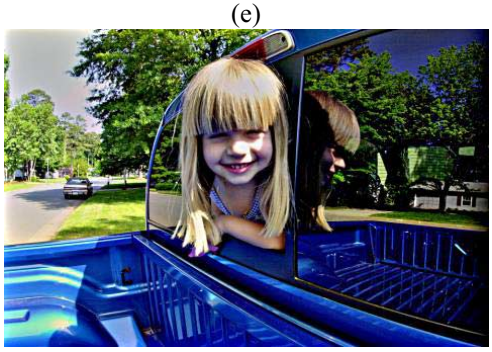

(f)

(g)

Fig. 7 The performance comparison: (a) the input image, (b) Conventional gamma correction (γ = 0.5), (c) Standard Histogram Equalization, (d) DRO, (e) AINDANE, (f) MSRCR, and (g) the proposed method (γ =0.5).

Fig. 8 shows another performance comparison for a low illuminance image. Fig. 8(a) shows the input image and Fig. 8(b) shows the output image processed by the GGC (γ=0.5), respectively. Although the GGC performs the acceptable visual quality, the lighting is inappropriately processed due to single curve correction. Although the GGC performs the acceptable visual quality, the lighting is inappropriately processed due to single curve correction.

(a)

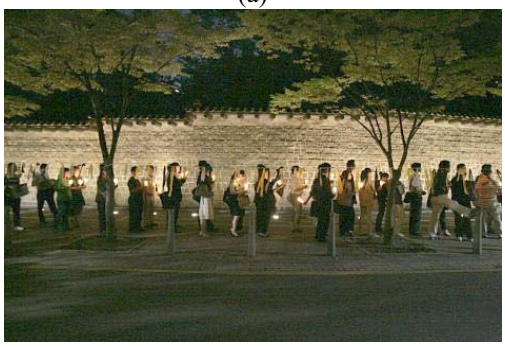

(b)

(c)

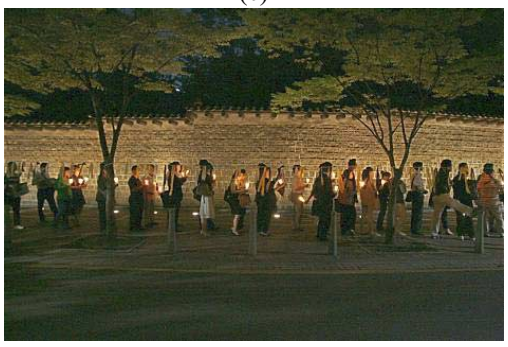

(d)

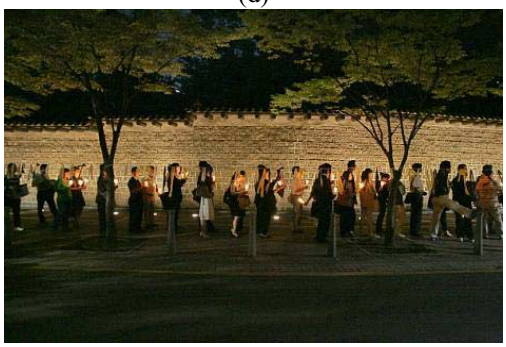

(e)

(f)

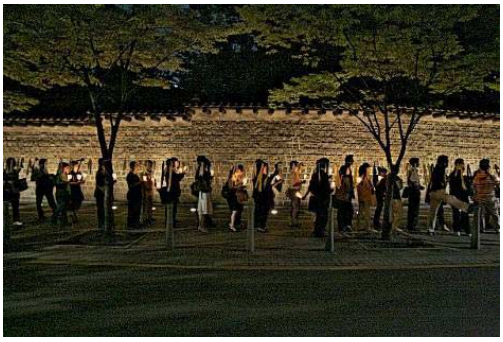

(g)

Fig. 8 The performance comparison: (a) the input image, (b) Conventional gamma correction (exponent = 0.5), (c) Standard Histogram Equalization, (d) DRO, (e) AINDANE, (f) MSRCR, and (g) the proposed method (exponent=0.5).

Fig. 8(c) shows the output image processed by the HE. Due to the lack of the color correction process, it gives the unnatural look as well as the decolorization. Fig. 8(d) shows the output image processed by the DRO. Although the brightness is enhanced, it gives the blurring and the contrast decreasing with the lack of the image enhancement method. Fig. 8(e) shows the output image processed by the AINDANE. The shadows and dark regions are appropriately enhanced in terms of details, features, and colors. The AINDANE performs the limited quality improvement owing to the global luminance enhancement. Fig. 8(f) shows the output image processed by the MSRCR. It gives the incorrect lightness and color noises. Fig. 8(g) shows the output image processed by the proposed method algorithm (γ=0.5). It shows the best enhancing result when compared with other algorithms in terms of overall brightness and contrast.

The proposed method was simulated with hundreds pictures containing different lighting conditions and scenes. When γ = 0.5, the image quality improvement was maximized. Fig. 9 shows a series of the image enhancing results of the proposed method. Fig. 9(a), Fig. 9(c) and Fig. 9(e) are the input images. Fig. 9(b), Fig. 9(d) and Fig. 9(f) are the output image processed by the proposed method. It can be noticed that the higher image quality was achieved.

(a)

(b)

(c)

(d)

(e)

(f)

Fig. 9 The image enhancing results without and with proposed method.

C. AMBE and Computational Time Comparison

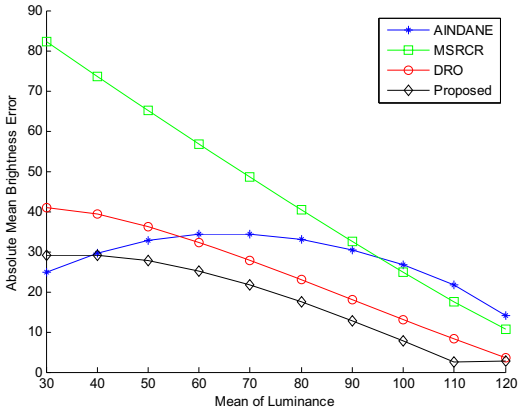

Fig. 10 The AMBE comparison.

In order to investigate the input/output brightness change of the image enhancing algorithms, we make use of the objective measure of Absolute Mean Brightness Error (AMBE) in [12]. This measure is defined as follows:

$$AMBE = \left| E_n(X) - E_n(Y) \right| \tag{11}$$

where *En(X)* is the average intensity of the input image *n* and *En(Y)* is the average intensity of the output image. The AMBE indicates the different average intensity between the input and the output. It can be seen that the lower AMBE minimizes the effect of the global contrast in the brightness property of the input image. Fig. 10 shows the AMBE comparisons of the proposed method and other enhancing algorithms (AINDANE /MSRCR/DRO) except for HE and gamma correction. The gray CZP patterns whose mean value ranges from 30 to 120 were simulated as to verify the luminance change from the input image to the output image. The MSRCR depicts the increasing AMBE as the illumination decreases due to the logarithmic operation unrelated with the brightness of the input image. When compared with the AMBE of the proposed method, the AINDANE without the local luminance information performs the higher AMBE in the luminance mean greater than 40 and the DRO using the single scale bilateral filter shows the higher AMBE in the luminance mean in overall. The proposed method maintains the best brightness loss overall and performs the lowest AMBE at the luminance mean 110.

We characterize the computational complexity of the proposed method with other enhancing algorithms (MSRCR/DRO/AINDANE) in Table I. The simulation platform is a PC environment, which has a CPU running at 2.8GHz and 2GB RAM. The AIDANE takes the least computation time due to the lack of the local luminance characteristic. Since the MSRCR calculates all spectral bands of the input image, additional computation times were required when compared with the proposed method. The DRO takes the most computation time to characterize the local luminance using the bilateral filter. The proposed method including the local luminance characterization approximately requires 23% of the DRO and 73% of the MSRCR in terms of the computational complexity.

TABLE I. The Comparison of Computational Time

Image Name and Resolution	Operation Time (msec) AINDANE	MSRCR	DRO	Proposed
People (600×400)	456	1,916	6,015	1,295
Red Hat Woman (768×512)	715	2,337	7,362	1,826
Door (1024×768)	1,202	3,996	12,984	2,815
Children (2000×1312)	3,554	16,307	49,981	12,281

IV. CONCLUSIONS

The color image enhancement method that makes use of the SVLM including the local brightness characteristic was presented. Combining the local characteristic effectively, the proposed method enhanced details of the input image as well as minimized loss of the edge sharpness in the non-uniform and low illumination conditions. The developed enhancement process resulted in the lowest AMBE when compared with AINDANE, MSRCR, and DRO. The down/up scaled Gaussian masking derived the benefit of the complexity reduction for the local brightness characterization. The proposed method also achieved the attractive computation saving when compared with the DRO and MSRCR.

ACKNOWLEDGMENT

This research was supported by Basic Science Research Program through the National Research Foundation of Korea (NRF) funded by the Ministry of Education, Science and Technology (2010-0017093).

REFERENCES

[1] G. W. Larson and H. Rushmeier, "A visibility matching tone reproduction operator for high dynamic range scenes," *IEEE Trans. Visualization and Computer Graphics*, Vol. 3, No. 4, pp. 165-188, Dec. 1997..

[2] T. Arich and S. Dikbas, " A Histogram Modification Framework and Its Application for Image Contrast Enhancement," *IEEE Trans. Image Processing*, Vol. 18, No. 9, pp 1921-1933, Sep. 2009

[3] W. Kao, J. Ye, M. Chu and C. Su, "Image Quality Improvement for Electrophoretic Displays by Combining Contrast Enhancement and Halftoning Techniques," *IEEE Trans. Consumer Electronics*, Vol. 55, No. 1, pp. 15-19, Feb. 2009.

[4] S. Battio, A. Castorina and M. Mancuso, "High dynamic range imaging for digital still camera: an Overview," *Journal of Electronics Imaging*, Vol. 12, No. 3, pp. 459-469, July 2003.

[5] J. A. Stark, "Adaptive image contrast enhancement using generalization of histogram equalization," *IEEE Trans. Image Processing*, Vol. 9, No. 5, pp. 889-896, May 2000.

[6] I. Park, T. Kim, J. Kim and B. Choi, "Data Driver Architecture and Driving Scheme of AMOLED Microdisplay for Mobile Projectors," *IEEE Trans. Consumer Electronics*, Vol.55, No.4, pp. 2365-2371, Nov. 2009

[7] A. Capra, A. Castorina and S. Corchs, "Dynamic Range Optimization by Local Contrast Correction and Histogram Image Analysis," *ICCE 2006*, pp. 309-310, Jan. 2006.

[8] L. Tao, "Adaptive and integrated neighborhood-dependent approach for nonlinear enhancement for color images," *Journal of Electronics Imaging*, Vol. 14, No. 4, pp. 1-14, Dec. 2005.

[9] D. J. Jobson, Z. Rahman and G. A. Woodell, "A Multiscale Retinex for Bridging the Gap Between Color Images and the Human Observation of Scenes," *IEEE Trans. Image Processing*, Vol. 6, No. 7, pp. 965-976, Jul. 1997.

[10] R. C. Gonzalez, *Digital Image Processing*, 3rd ed., Addison Wesley Longman, 2007.

[11] J. Ha, S. Lee, T. Kim, W. Choi and B. Kang, "A New Approach to Color Adjustment for Mobile Application Display with a Skin Protection Algorithm on a CIE1931 Diagram," *IEEE Trans. Consumer Electronics*, Vol. 53, No. 1, pp. 191-196, Feb. 2007.

[12] P. Rajavel, "Image Dependent Brightness Preserving Histogram Equalization," *IEEE Trans. Consumer Electronics*, Vol. 56, No. 2, pp. 756-763, May. 2010

BIOGRAPHIES

Sungmok Lee received the B.S and M.S. degrees in electronic engineering from Dong-A University, Busan, Korea, in 2005 and 2007, respectively. He is currently working toward his Ph.D. degree at the university. His research interests include digital camera processing systems, VLSI architecture design and image processing.

Homin Kwon received the B.S. and M.S. degrees in electronics engineering from Dong-A University, Busan, Korea in 2002 and 2004, respectively, and the Ph.D. degree from Arizona State University in 2009. While at ASU, he worked and published in J-DSP, acoustic sensing in wireless sensor networks and voice scene characterization. He had held summer internship appointments at DynaSig Co. in 2006-2007. He is a senior research engineer at TruDef Research, Inc. where his work focuses on the region of interest based video quality improvements and image enhancement algorithms.

Hag-Yong Han received the B.S., M.S. and Ph.D. degrees in electronics engineering from Dong-A University, Busan, Korea, in 1994, 1998 and 2004, respectively. He had worked as Chief of R&D at the Easy Harmony Co. Ltd., Busan, Korea, in 2001, and a post doctoral researcher at the Pusan National University, Busan Korea, in 2006-2007, respectively. He now is the research professor of the Multimedia Research Center of the Dong-A University. His research interests include pattern recognition, audio / image / video processing, DSP application

Gidong Lee received the B.S., M.S. and Ph.D. degrees in electronics engineering from Pusan National University, Busan, Korea, in 1989, 1991 and 2000, respectively. He had worked at LCD R&D center in Samsung SDI, Korea, in 1991-1997, and a Research Fellow at Liquid Crystal Institute, Kent State University, USA, in 2001-2003, respectively. Since 2004, he has been with the department of electronics engineering, Dong-A University, Busan, Korea. His research interests include display devices.

Bongsoon Kang received the B.S. degree in Electronics Engineering from Yonsei University, Seoul, Korea, in 1985, and the M.S. degree in Electrical Engineering. from University of Pennsylvania, Pennsylvania, USA, in 1987, and the Ph.D. degree in Electrical and Computer Engineering from Drexel University, Philadelphia, USA, in 1990. From Dec. 1989 to Feb. 1999, he had worked as a senior staff researcher at Samsung Electronics Co. Ltd., Kihung, Korea. Since March 1999, he has been with the Department of Electronic Engineering, Dong-A University, Busan, Korea. He is the director of the Multimedia Research Center of the university. His research interests include image processing, hardware architecture designs, and wireless communications. He was honored as a 2007 winner of the Chester Sall Award for the 1st place best paper in the IEEE Transactions on Consumer Electronics on Jan. 2009.